Eur. Radiol. 9, 652–661 (1999)

European Radiology

Original article

MRI of bone marrow: opposed-phase gradient-echo sequences with long repetition time

M. Seiderer*, A. Staebler[1], H. Wagner[2]

[1] Department of Radiology, Klinikum Grosshadern, University of Munich, Marchioninistrasse 15, D-81366 Munich, Germany
[2] Department of Pathology, Klinikum Grosshadern, University of Munich, Marchioninistrasse 15, D-81366 Munich, Germany

Received: 23 May 1997; Revision received: 3 March 1998; Accepted: 31 July 1998

Abstract. Signal intensity for opposed-phase gradient-echo (GE) sequences of tissues composed of fat- and water-equivalent cells such as red bone marrow is extremely sensitive to variation of the ratio of both cell populations (fat-to-water ratio $Q_{F/W}$). Because most bone marrow pathology results in variation of $Q_{F/W}$, GE sequences are characterized by high-contrast imaging of pathology. The aim of this study was to evaluate the influence of TR, TE, FA, $Q_{F/W}$ and histology on signal intensity. Signal intensity of opposed-phase GE sequences as a function of TR, TE, FA, and $Q_{F/W}$ was measured for a fat-water phantom and cadaver specimens of normal bone marrow (red and yellow) and pathological bone marrow (tumors). All specimens were correlated to histology. Opposed-phase GE imaging of red bone marrow pathology results in low-signal-intensity imaging of intact red bone marrow and high-signal-intensity positive contrast imaging of pathology associated with a change in $Q_{F/W}$. In first-order approximation the signal intensity of pathology is linearly correlated to the change in $Q_{F/W}$. Opposed-phase GE imaging is a sensitive imaging technique for red bone marrow pathology. Relative contrast of red bone marrow pathology is similar to fat-suppressed imaging techniques. Acquisition time is identical to T1-weighted SE sequences.

Key words: Gradient-echo sequence – Chemical-shift imaging – Bone marrow

Correspondence to: M. Seiderer

**Present address:* Radiologie am Prinzregentenplatz, Prinzregentenplatz 13, D-81675 München, Germany

Introduction

Gradient-echo sequences with longer repetition times than used for fast imaging (TR ≥ 100 ms) and echo times (TE) adjusted to anti-parallel transverse magnetization of fat and water protons (opposed-phase sequences) which are sensitive to chemical shift have proved to be of high diagnostic sensitivity for imaging of bone marrow pathology. The main advantage is the low signal intensity of red bone marrow and the high signal intensity of pathology such as tumor, inflammatory disease, and edema, all of which results in a lesion-to-marrow contrast which typically exceeds that for T1- and T2-weighted SE imaging. Although described by Wismer et al. [1] and widely diagnostically used, no systematic data which relates the signal intensity of mixed fat-water tissues (fat cells, water-equivalent cells, extracellular fluid) to imaging parameters [TR, TE, flip angle (FA)] and tissue parameters, especially the fat-to-water ratio $Q_{F/W}$, have been reported in the literature thus far.

Chemical shift

The majority of protons in biological tissues are bound either in water via an OH-binding (water-bound or water-equivalent protons) or in fat (fat-bound or fat-equivalent protons) via CH_2-binding of the long fatty acid chains. Due to shielding effects of the hull electrons, the protons experience different magnetic fields and thus precess with different frequencies which are 3.5 ppm apart. Imaging relevant phase shift between fat- and water-bound protons is visualized by all GE sequences and special SE-based sequences (e.g., Dixon technique; Fig. 1). The phase shift between fat and water results in a TE-dependent modulation of signal intensity for all pixels containing fat- and water-bound protons. Signal intensity is dependent both on TE and magnetic field strength B_o. For in-phase imaging transverse magnetization of fat-bound and water-bound protons is add-

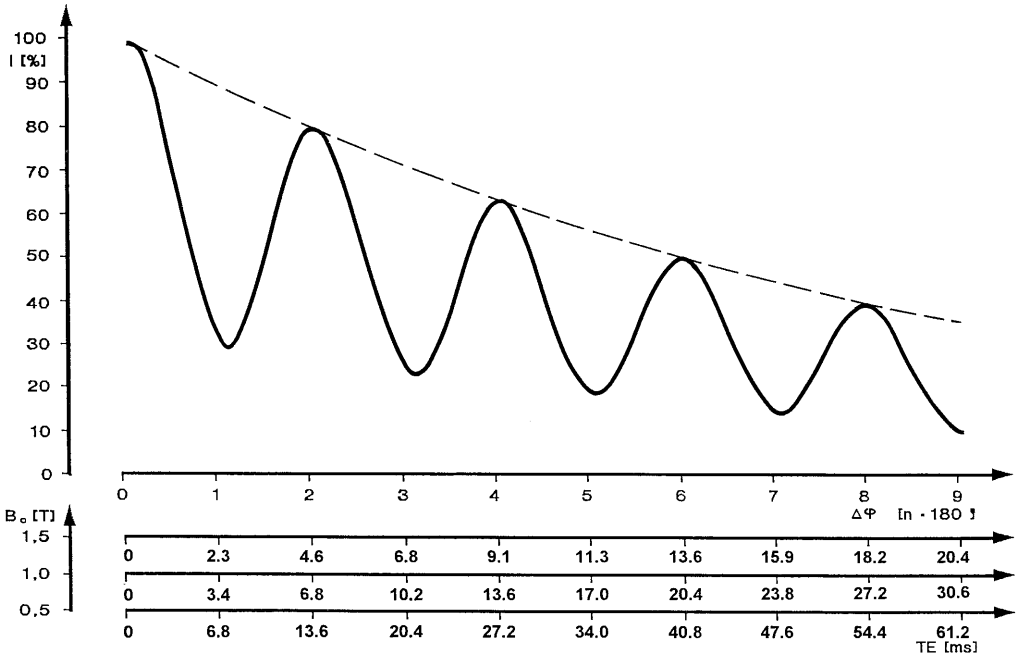

Fig. 1. Chemical-shift-induced signal intensity modulation for gradient-echo (GE) sequences as a function of TE ($M_{xy\text{-}fat} \neq M_{xy\text{-}water}$). Signal intensity modulation is caused by vector addition of transverse magnetization of fat- and water-bound protons. The maximum values of the curve are characterized by the T2* signal intensity decay of transverse magnetization and are not influenced by chemical shift effects and are independent from $Q_{F/W}$. For $M_{xy\text{-}fat} = M_{xy\text{-}water}$ all opposed-phase signal intensity minima would be zero. For $M_{xy\text{-}fat} \neq M_{xy\text{-}water}$ as in the case shown the signal intensity minima are given by the residual transverse magnetization (difference of fat and water magnetization)

Table 1. Frequency shift (Δν), fat-water cycle time and opposed-phase GE-imaging echo times (TE) for the first four opposed-phase cycles ($\pi + 2n \cdot \pi$; $n = 0$–4) as a function of the magnetic field strength B_o

B_o (T)	Δν (1/s)	Cycle time (ms)	TE (ms)				
			$n = 0$	$n = 1$	$n = 2$	$n = 3$	$n = 4$
0.20	29.4	34.0	17.0	51.0	85.0	119.0	153.1
0.35	51.5	19.4	9.7	29.2	48.6	68.0	87.5
0.50	73.5	13.6	6.8	20.4	34.0	47.6	61.2
1.00	147.0	6.8	3.4	10.2	17.0	23.8	30.6
1.50	220.5	4.5	2.3	6.8	11.3	15.9	20.4

ed and thus is maximized as for SE imaging (Fig. 2 a, b). For a TE where the transverse fat and water magnetization is opposite in direction (opposed-phase imaging) magnetization is the difference of both magnetization components and thus signal intensity is minimized (Fig. 2 c, d).

The frequency shift of 3.5 ppm between water- and fat-bound protons is linked via the magnetic field strength B_o to the Larmor frequency and thus the precession frequency of the protons [1]. The TE for in-phase or opposed-phase imaging is dependent on B_o and the phase shift Δφ selected. Echo time is shorter the higher the B_o [2] and the smaller the number of fat-water cycles [3, 4].

$$TE = \Delta\varphi/\Delta\nu$$
$$\Delta\nu = 3.5 \cdot 10^{-6} \cdot \omega/2\pi$$
$$\Delta\varphi = 3.5 \cdot 10^{-6} \cdot TE \cdot \omega/2\pi$$
$$\omega = \gamma \cdot B_o \quad (1)$$

$$TE = 2\pi \cdot \Delta\varphi/3.5 \cdot 10^{-6} \cdot \gamma \cdot B_o \quad (2)$$

$$\text{Opposed phase: } \Delta\varphi_{I\text{-}min} = \pi + n \cdot 2\pi \; (n = 0, 1, 2, 3, \ldots) \quad (3)$$

$$\text{In phase: } \Delta\varphi_{I\text{-}min} = n \cdot 2\pi \; (n = 0, 1, 2, 3, \ldots) \quad (4)$$

where TE is echo time, Δφ is chemical-shift-related phase difference, ω is Larmor frequency, Δν is chemical-shift-related frequency difference, E is resonance energy, γ is gyromagnetic ratio, and B_o is magnetic field strength.

Opposed-phase imaging occurs at cyclic phase differences for fat- and water-bound protons of π [3], and in-phase imaging at phase differences of 0 [4]. For $B_o = 1.0$ T and a frequency difference Δν of 147 1/s the cycle time TE is 6.8 ms (Table 1). Thus, TE for opposed-phase imaging is 3.4, 10.2, 17.0, and 23.8 ms, and TE for in-phase imaging 6.8, 13.6, 20.4, and 27.2 ms. As the difference in precession frequency between fat- and water-bound protons increases with B_o, the TE cycle time and the minimum TE for opposed-phase and in-phase imaging decreases (Table 1).

Materials and methods

Measurements were carried out on a 1.0-T whole-body imager with an effective $B_o = 0.96$ T (Magnetom, Siemens, Erlangen, Germany). Acquisition time for each sequence was chosen to assure appropriate signal-to-noise ratios.

For the evaluation of the influence of the fat-to-water ratio $Q_{F/W}$ and the TE on signal intensity for spoiled opposed-phase GE sequences (FLASH technique) two separate experiments were performed. Based on the results of measurements on a fat-water phantom with linear variation of $Q_{F/W}$ measurements were verified on MR images of cadaver specimens (femur, spine) of normal red and yellow bone marrow and red marrow pathology (metastasis, leukemia) and correlated to histology. All measurements also were correlated to SE sequences using identical TR and TE.

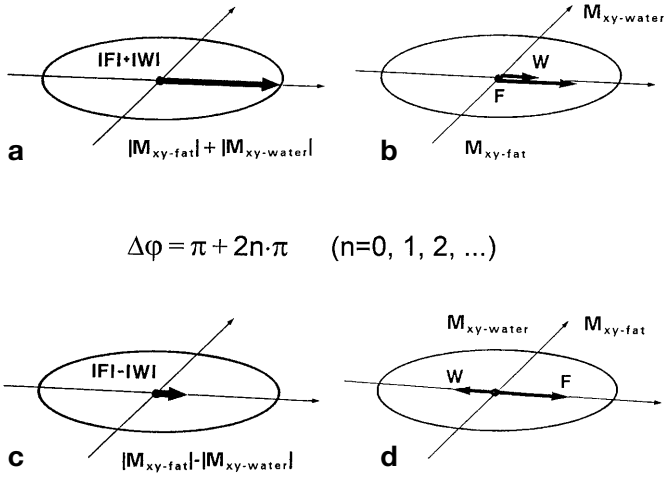

Fig. 2 a–d. Echo-time-dependent signal intensity modulation for GE imaging of voxels containing fat- and water-equivalent spins. Minimum and maximum signal intensity by vector addition of tranverse magnetization of fat- and water-bound protons at the time of signal intensity readout (TE). The phase difference of fat- and water-bound protons is caused by a difference in precession frequency of 3.5 ppm. **a, b** Maximum signal intensity for in-phase imaging (addition of magnetization of fat- and water-bound protons; **a** imaging relevant magnetization vector, **b** transverse magnetization components). **c, d** Minimum signal intensity for opposed-phase imaging (subtraction of magnetization of fat- and water-bound protons; **c** imaging relevant magnetization vector, **d** transverse magnetization components). Parts **a** and **b** represent the only condition for magnetization of spin-echo (SE) sequences (rephasing of phase differences at time of signal intensity readout (TE))

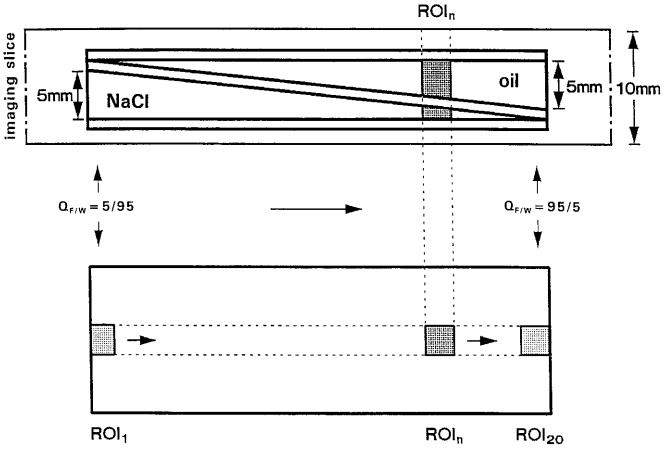

Fig. 3 a, b. Wedge-shaped fat-water phantom. **a** Projection view from the side (parallel to the imaging slice). **b** Imaging view of the phantom (90° rotated to **a**). Measurement of the fat-to-water ratio for values between $5/95 < Q_{F/W} < 95/5$ by sliding the region-of-interest from left to right

Fat-water phantom

For continuous variation of $Q_{F/W}$ a dual-chamber glass phantom with two separate and opposed-oriented wedge-shaped fluid chambers, one filled with olive oil and one filled with Gd-DTPA (0.1 mmol/l) doped saline, was used (Fig. 3) [2]. According to the geometry, there was a linear change in $Q_{F/W}$ from one end of the long axis of the phantom to the other. This model allowed for elimination of susceptibility effects and identical voxel geometry for all values of $Q_{F/W}$.

For signal intensity evaluation of the fat-water phantom a single in-plane slice with a slice thickness of 10 mm covering the whole phantom in plain, a field of view of 105 mm, and an image matrix of 256 × 256 pixels was acquired. Signal intensity of different $Q_{F/W}$ values was measured by placing 20 continuous, square-formed regions of interest of 4 × 4 mm (100 pixels) along the phantom (Fig. 3); thus, signal intensity for $Q_{F/W}$ values ranging from $5/95 \le Q_{F/W} \le 95/5$ (5–95% oil, 95–5% water) in steps of 5% each was obtained. $Q_{F/W} = 0/100$ (water-bound protons only) and $Q_{F/W} = 100/0$ (fat-bound protons only) were measured by filling both chambers of the phantom with one kind of fluid only.

To evaluate the influence of the TE on signal intensity, TE was varied for GE sequences from 11 to 22 ms and for SE sequences from 13 to 22 ms in steps of 1 ms each. To allow for a direct comparison of GE and SE sequences, FA was 90° with TR = 500 ms.

Autopsy specimens

Ten bone marrow space specimens of trabecular bone (vertebral body, femoral head) were examined, six normals (red and yellow bone marrow) and four with metastasis or leukemia (acute myelogenous leukemia, chronic myelogenous leukemia, acute lymphatic leukemia, metastasis of carcinoma of the prostate). To evaluate the diagnostic potential of spoiled GE sequences for high-contrast imaging of red bone marrow pathology, signal intensity for a wide variation of acquisition parameters, TR, TE, and FA, was measured by a region of interest adapted in size to anatomical demands. The TE for GE and SE sequences was varied between 13 and 20 ms (increment 1 ms), TR between 100 and 900 ms (increment 200 ms), and FA between 10 and 90° (increment 20°). Thus, for GE imaging a total of 200 different sequences was used for all cadaver specimens. The total number for SE sequences was 40 (no variation in FA). Related to the actual field strength of the imager of $B_o = 0.96$ T (nominal $B_o = 1.0$ T), a TE of 14 and 21 ms corresponded to in-phase imaging and a TE of 10 and 17 ms to opposed-phase imaging.

Results

Fat-water phantom

Signal intensity for spoiled GE and SE sequences as a function of $Q_{F/W}$ and TE is shown in Fig. 4 as projective 3D data.

For GE sequences there is pronounced signal intensity modulation dependent on TE and $Q_{F/W}$. For TE values of 11 and 17 ms which correspond to opposed-phase transverse magnetization there is almost complete neutralization of transverse magnetization of fat- and water-bound protons ($M_{xy\text{-}fat} = -M_{xy\text{-}water}$) resulting in signal intensity close to zero. Signal intensity decreases si-

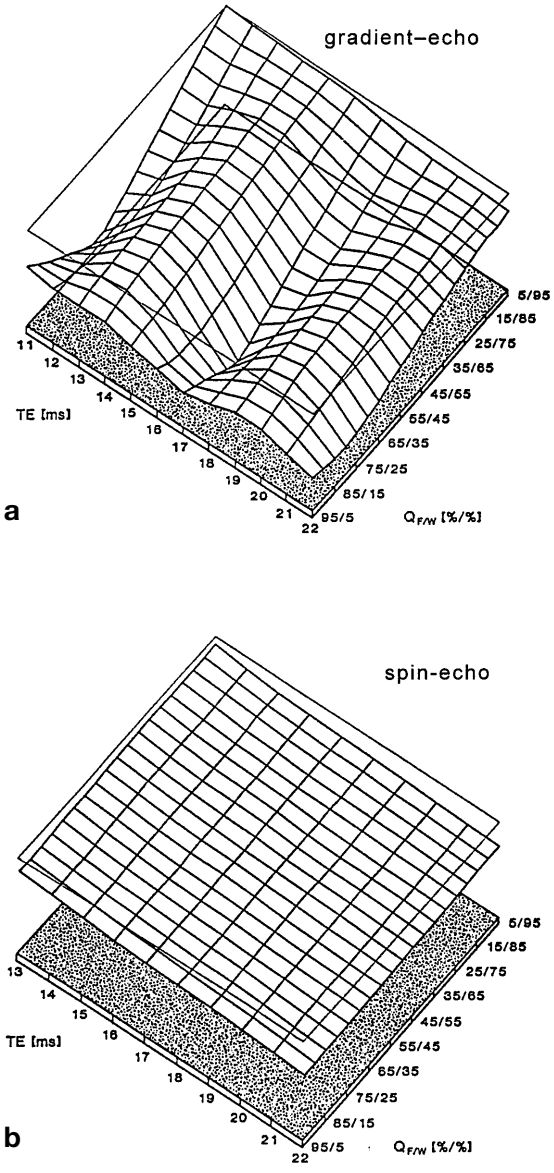

Fig. 4 a, b. Projected 3D signal intensity data for the fat-water phantom as a function of the fat-water ratio $Q_{F/W}$ and TE (B_o = 1.0 T) [*rectangular frame* maximum signal intensity of all parameter combinations (TE, $Q_{F/W}$)]. **a** GE sequences: pronounced signal intensity modulation at TE values equivalent to subtraction of fat- and water-magnetization (opposed-phase imaging) (TE = 11 and 17 ms). Minimum of signal intensity close to zero for $Q_{F/W}$ = 70/30 (identical fat- and water-magnetization). Maximum of signal intensity for in-phase imaging (TE = 14 and 20 ms). Linear increase in signal intensity from $Q_{F/W}$ = 70/30 both to $Q_{F/W}$ = 0/100 (water-bound protons only) and $Q_{F/W}$ = 100/0 (fat-bound protons only) for all TE values corresponding to out-of-phase imaging (except in-phase imaging at TE = 14 and 20 ms, identical to SE imaging). **b** SE sequences: linear variation in signal intensity with TE and $Q_{F/W}$ without signal intensity modulation

nusoidally the more TE approaches opposed-phase transverse magnetization ($|M_{xy\text{-}fat}| = |M_{xy\text{-}water}|$).

For a change in $Q_{F/W}$ from minimum signal intensity ($M_{xy\text{-}fat} = -M_{xy\text{-}water}$, opposed-phase TE, $Q_{F/W}$ = 70/30) to signal intensity of pure water ($Q_{F/W}$ = 0/100) or pure fat ($Q_{F/W}$ = 100/0), there is a linear increase in signal intensity with $Q_{F/W}$. The opposed-phase $Q_{F/W}$ for minimum signal intensity ($Q_{F/W}$ = 70/30) is given by the specific signal intensity of the fat-bound (olive oil) and water-bound (Gd-DTPA doped saline) protons. The cyclic repetition of minimum signal intensity for a prolongation of TE from 11 to 17 ms is in accordance with the theoretical TE values for π phase shifts for transverse fat- and water magnetization (Table 1).

For SE sequences no signal intensity modulation with variation of TE or $Q_{F/W}$ occurs. Signal intensity differences for distinct $Q_{F/W}$ values are linear with variation of $Q_{F/W}$ between the values for pure water and fat (monosubstances). The exponential T2 signal intensity decay is relatively small within the TE range under investigation and linear with TE to first order. The same applies to GE sequences, even with the faster signal intensity decay by T2* compared with T2. For GE sequences signal intensity modulation for opposed-phase TE values and $Q_{F/W}$ values resulting in significant signal intensity attenuation by far override the relaxation time effects relevant for SE sequences.

The fat-water phantom results indicate a linear increase in signal intensity from zero for a tissue-specific $Q_{F/W}$ with identical transverse magnetization of the fat and water protons (D in Fig. 5) either to water (D → C, D → B, D → A) or to fat (D → E, D → F, D → G). For different specific signal intensity of fat- and water-bound protons [I = f (M_o, T1, T2, T2*, TR, TE, FA)] zero signal intensity is related to $Q_{F/W}$ according to Eq. (5):

$$I_{spec\text{-}F} \cdot Q_{F/W} = I_{spec\text{-}W} \cdot (1\text{-}Q_{F/W}) \quad (5)$$

$$\Delta I/\Delta Q_{F/W} = (I_{spec\text{-}F} + I_{spec\text{-}W})/100, \quad (6)$$

where $I_{spec\text{-}F}$ is specific signal intensity of fat-equivalent cells (monosubstance; $Q_{F/W}$ = 100/0), $I_{spec\text{-}W}$ is specific signal intensity of water-equivalent cells (monosubstance; $Q_{F/W}$ = 0/100), $Q_{F/W}$ is fat-to-water ratio (0/100 ≤ $Q_{F/W}$ ≤ 100/0 ≡ 0 ≤ $Q_{F/W}$ ≤ 1), and I is image-relevant signal intensity.

The imaging relevant GE signal intensity can be calculated from the gradient of the signal intensity I ($\Delta I/\Delta Q_{F/W}$) by Eq. (6). This gradient is exclusively dependent on the signal intensity for both monosubstances ($Q_{F/W}$ = 100/0 and $Q_{F/W}$ = 0/100) and is proportional to the sum of the signal intensities [6]. The signal intensity gradient (slope of the curve) on either side of D is identical in size (Fig. 5) and is independent of the specific signal intensity of the fat- and the water-equivalent cells.

Autopsy specimens

Mixed fat-water tissues

The signal intensity of spoiled GE sequences for histologically correlated cadaver specimens of normal red and yellow bone marrow and different tumor types as a function of TE and $Q_{F/W}$ (FA = 90°) is shown in Figs. 6 and 7.

Regarding $Q_{F/W}$ all tissues with 40/60 < $Q_{F/W}$ < 60/40 (40–60 % fat; red bone marrow, acute myelogenous leu-

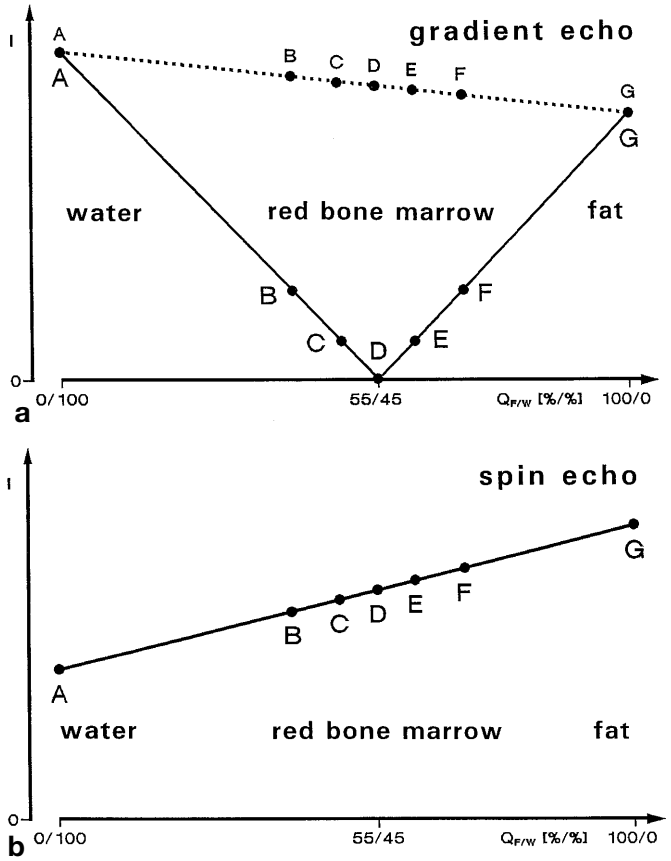

Fig. 5 a, b. Signal intensity for fat-water tissues imaged by spoiled opposed-phase GE and T1-weighted SE sequences as a function of the fat-to-water ratio $Q_{F/W}$ taking into account relaxation time and proton-density-related tissue-specific (I_{spec}) signal intensity differences between fat- and water-equivalent mono-substances (e.g., $Q_{F/W}$ = 100/0: yellow bone marrow; $Q_{F/W}$ = 0/100: tumor) (GE: $I_{spec\text{-}fat} = 0.8 \cdot I_{spec\text{-}water}$; SE: $I_{spec\text{-}fat} = 2.0 \cdot I_{spec\text{-}water}$). **a** Opposed-phase GE sequences: linear signal intensity increase *(solid line)* starting from zero signal intensity *(D)* and cumulating on either side from *D* to the maximum signal intensity specific for water- ($Q_{F/W}$ = 0/100) *(A)* and fat-specific ($Q_{F/W}$ = 100/0) *(G)* mono-substances. The gradient of the slopes on either side is identical but opposite in sign. The $Q_{F/W}$ for zero signal intensity (*D*; Eq. (5)) is equivalent to the ratio of the specific signal intensity of the mono-substances (in this example: $I_{spec\text{-}fat}/I_{spec\text{-}water} = 1.0/0.8 = 1.25 \approx Q_{F/W} = 45/55$). *B*, *C*, *E* and *F* stand for the signal intensity of mixed fat-water tissues (see text). In-phase GE sequences *(dotted line)* are characterized by a linear signal intensity change with $Q_{F/W}$ and identical signal intensity to opposed-phase GE sequences for fat- and water-equivalent mono-substances (*A* $Q_{F/W}$ = 0/100, *G* $Q_{F/W}$ = 100/0) (neglecting TE-related signal intensity loss due to different TEs for opposed-phase and in-phase imaging). No signal intensity modulation with $Q_{F/W}$. Relatively small signal intensity differences for tissues with $Q_{F/W}$ = 100/0 *(G)* and $Q_{F/W}$ = 0/100 *(A)* related to similar specific signal intensity for fat- and water-equivalent tissues. **b** SE sequences: identical to in-phase GE sequences linear signal intensity change with $Q_{F/W}$. According to different specific signal intensity for fat- and water-equivalent tissues (different T1) there is pronounced signal intensity difference between fat- and water-equivalent tissues (*A* $Q_{F/W}$ = 0/100, *G* $Q_{F/W}$ = 100/0), by far exceeding the values for opposed-phase and in-phase GE sequences (TR ≥ 100 ms; $A \rightarrow G$, $G \rightarrow A$). As for in-phase GE sequences, there is no signal intensity modulation with $Q_{F/W}$, although signal intensity differences for mono-substances are relatively small for GE imaging. Signal intensity differences between mixed fat-water tissues such as red bone marrow and fat-equivalent tissues ($B \rightarrow G$, $C \rightarrow G$, $D \rightarrow G$, $E \rightarrow G$, $F \rightarrow G$) or water-equivalent tissues ($B \rightarrow A$, $C \rightarrow A$, $D \rightarrow A$, $E \rightarrow A$, $F \rightarrow A$), are larger due to signal intensity modulation by subtraction of transverse fat- and water-magnetization

kemia) presented with a pronounced decrease in signal intensity for opposed-phase GE imaging (TE = 17 ms) compared with in-phase imaging. For yellow bone marrow and tumors with $Q_{F/W}$ > 95/5 there was no $Q_{F/W}$-related signal intensity drop (Fig. 6).

The residual signal intensity for opposed-phase imaging of red bone marrow compared with in-phase imaging for all sequences examined (100 ms ≤ TR ≤ 900 ms, 10° ≤ FA ≤ 90°) was relatively low with values between 27.9 % (TR/FA = 300 ms/90°) and 32.6 % (TR/FA = 500 ms/30°). The global average signal intensity for all five TR values and all five FA values was 30.7 ± 1.3 % (mean ± SD) equivalent to a reduction in signal intensity for red bone marrow of 69.3 ± 1.3 % compared with in-phase GE imaging. There was a slight, although not statistically significant, trend for an increase in signal intensity for longer TR and lower FA values (paired *t*-test; $p < 0.05$).

For tissues with either a high fat content, such as yellow bone marrow ($Q_{F/W}$ > 95/5), or a dominance of water-bound protons, such as tumors ($Q_{F/W}$ < 5/95), there was no signal intensity modulation with TE (Fig. 6). Residual signal intensity for opposed-phase (TE = 17 ms) compared with in-phase imaging (TE = 14 ms) for tumors with complete replacement of fat cells was 87.5 ± 1.8 % for all parameter combinations of TR and FA examined. Compared with the signal intensity of red bone marrow pathology with $Q_{F/W}$ < 5/95, the signal intensity of intact red marrow was 35.0 % on average, which is equivalent to a lesion-to-marrow signal intensity ratio of 2.85. The lowest signal intensity ratio was 2.62 (TR = 700 ms, FA = 10°), the largest 3.23 (TR = 300 ms, FA = 90°). There was a slight trend for a decrease in signal intensity ratios with increasing TR and a more pronounced trend for an increase with increasing FA.

Contrary to GE sequences, there was no $Q_{F/W}$-related signal intensity drop for red bone marrow with SE sequences comparing a TE of 17 and 14 ms. The relative signal intensity reduction was discrete both for red bone marrow as well as pathology and compares to the values for tumor or yellow bone marrow in opposed-phase GE imaging. The mean signal intensity for TE = 17 ms compared with 14 ms (TR = 100–900 ms) was 92.6 ± 2.7 % (mean ± SD) for red bone marrow and 92.5 ± 2.4 % for tumors. The corresponding results for tumors imaged with opposed-phase GE sequences (TR = 100–900 ms) was 89.4 ± 0.6 % indicating a faster signal intensity decay by T2* instead of T2 for SE sequences.

The dominant influence of $Q_{F/W}$ as imaging parameter for low signal intensity imaging of red bone marrow over spin density and relaxation times was demonstrated by the cadaver specimen of a patient with acute myelogenous leukemia and replacement of red bone marrow hematopoietic cells by tumor cells but preservation of fat cells (Figs. 7, 8). This case presents with a signal intensity drop for opposed-phase compared with in-phase GE imaging identical to red bone marrow, whereas all other histologically verified tumor cases presented with loss of signal intensity drop due to complete replacement of red bone marrow by tumor cells (replacement of hematopoietic cells and fat cells).

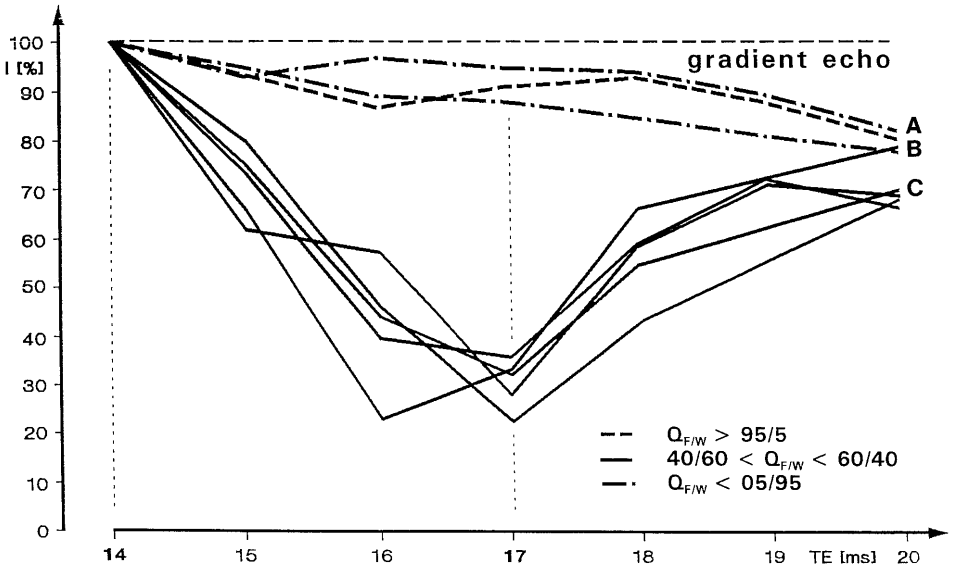

Fig. 6. Signal intensity modulation for bone marrow space tissues for GE sequences as a function of histologically determined $Q_{F/W}$ and TE ($I_{TE = 14\,ms}$ = 100 %; TR/FA = 500 ms/90°). Pronounced signal intensity modulation for bone marrow space tissues with 40/60 < $Q_{F/W}$ < 60/40 (red bone marrow and tumor [*C* acute myelogenous leukemia (compare Fig. 7)]. For opposed-phase GE imaging (TE = 17 ms) signal intensity reduction is between 62.4 and 77.1 % (TR/FA = 500 ms/90°) as compared with in-phase imaging (TE = 14 ms). No TE-related signal intensity modulation for tissues with $Q_{F/W}$ > 95/5 (yellow bone marrow) and $Q_{F/W}$ < 5/95 [tumor: *A* chronic myelogenous leukemia; *B* cancer of the prostate (compare Fig. 7)]

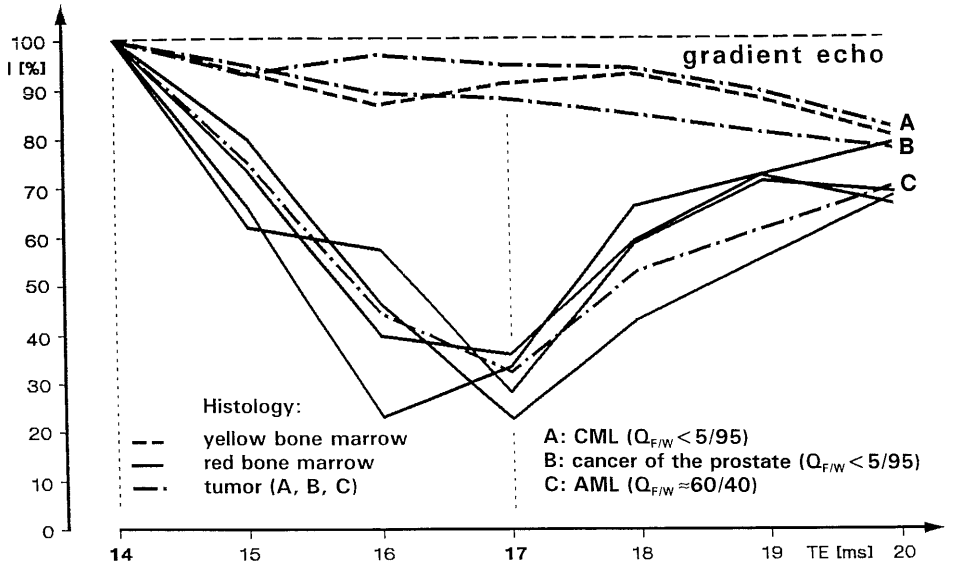

Fig. 7. Signal intensity modulation of bone marrow space tissues for GE sequences related to histology and TE ($I_{TE = 14\,ms}$ = 100 %) (TR/FA = 500 ms/90°). Red bone marrow (40/60 < $Q_{F/W}$ < 60/40) and pathologic tissue with a comparable $Q_{F/W}$ (acute myelogenous leukemia without replacement of fat cells by tumor cells) present with identical TE-related signal intensity modulation. Compared with tissues which mainly contain fat (yellow bone marrow; $Q_{F/W}$ > 95/5) or pathologies which do not contain fat cells (metastasis of carcinoma of the prostate, chronic myelogenous leukemia; $Q_{F/W}$ < 5/95) normal red bone marrow is imaged with low signal intensity. Thus, yellow marrow and almost all pathology (replacement of red bone marrow fat cells) is imaged with positive contrast. Pronounced signal intensity modulation for tissues with 40/60 < $Q_{F/W}$ < 60/40. For opposed-phase GE imaging (TE = 17 ms) signal intensity decrease is between 62.4 and 77.1 % (TR/FA = 500 ms/90°) as compared with in-phase imaging (TE = 14 ms). No TE-related signal intensity modulation for tissues with $Q_{F/W}$ > 9/5 and $Q_{F/W}$ < 5/95

Fat- and water-equivalent tissues

Tissues with a major predominance of either fat- or water-equivalent cells are imaged by GE sequences, regardless of TE, qualitatively as with SE sequences (identical imaging parameters, susceptibility, diffusion, and partial saturation neglected). Neither for yellow bone marrow nor for tumors of the bone marrow space with a total replacement of fat cells by tumor cells does signal intensity modulation with variation of TE occur (Figs. 4, 6).

The average residual signal intensity for opposed-phase GE (TE = 17 ms) compared with in-phase imaging (TE = 14 ms) for TR = 100–900 ms and FA = 10–90° for tumor was between 84.2 ± 6.4 % (TR/FA = 900 ms/10°) and 90.1 ± 4.4 % (TR/FA = 500 ms/90°). The mean signal intensity for all TR and FA values (25 pairs of parameters) was 87.5 ± 1.8 %. The average drop in signal intensity compared with TE = 14 ms was 12.5 ± 1.8 %. This was only 18 % of the signal intensity

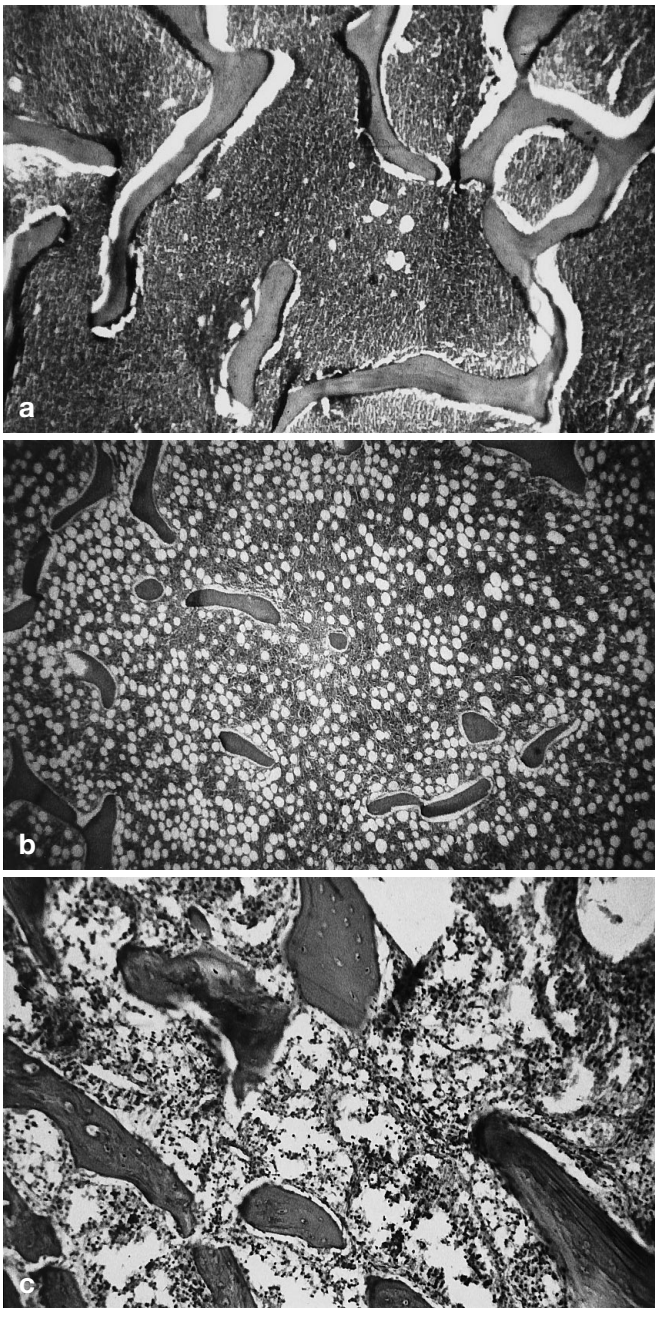

Fig. 8a–c. Histologic specimens of tissues and pathologies examined. **a** Chronic myelogenous leukemia. Total replacement of red bone marrow (marrow-specific cells and fat cells) by myelogenous cells (magnification × 220). **b** Acute myelogenous leukemia. Replacement of hematopoietic cells by myelogenous cells. Preservation of fat cells (magnification × 90). **c** Osteoblastic metastasis in cancer of the prostate. Total replacement of yellow bone marrow by necrotic tumor cells. Trabecular hyperplasia (magnification × 220)

drop which was measured for red bone marrow for opposed-phase compared with in-phase imaging and is mainly caused by T2* decay. These results indicate that tumors with substitution of fat cells by tumor cells, regardless of TR and FA, present only with a negligible signal intensity drop comparing in-phase and opposed-phase GE sequences and thus are imaged with high contrast to red bone marrow.

As for red bone marrow for tumors, there was no statistically significant change in signal intensity with longer TR (paired *t*-test); however, there was a trend for an increase in signal intensity with an increase in FA. The average signal intensity (all TR values) increased steadily from 85.6 ± 1.3 % for FA = 10 ° to 89.4 ± 0.6 % for FA = 90 °. Although there was a statistically significant difference for FA = 10 ° ($p < 0.01$) and FA = 30 ° ($p < 0.05$) compared with the FA = 90 ° values, this maximum difference in signal intensity was 3.8 % only and therefore can be ignored compared with the chemical-shift-induced signal intensity changes for opposed-phase GE imaging of red bone marrow.

As for red bone marrow, there was no signal intensity modulation for SE sequences with TE. Signal intensity decay with prolongation of TE exclusively was exponential by T2. Due to the longer T2 for SE imaging as compared with T2* for GE imaging, signal intensity for TE = 17 ms (90.6 ± 1.6 %) was higher than for opposed-phase GE imaging (87.5 ± 1.8 %; mean values for TR = 100–900 ms).

Contrast-to-noise ratio

The results for the contrast-to-noise ratios (CNRs) for the model of tumor in red bone marrow (metastasis) for in-phase GE, opposed-phase GE, and SE sequences are listed in Tables 2–4. The most important difference is a positive lesion-to-marrow contrast for GE sequences and a negative contrast for SE sequences. Moreover, CNR for opposed-phase GE sequences exceeds CNR for in-phase GE sequences for all parameter combinations (TR, FA) measured and CNR maximum values of GE sequences exceed CNR values of SE sequences (opposite sign).

Contrast for opposed-phase GE sequences (TE = 17 ms) was highest for TR = 900 ms and FA = 90 ° (Table 2). For all flip angles except FA = 10 ° there was an increase in CNR with TR. With higher FA values the increase was more pronounced with higher TR values, whereas for FA = 30 ° there was only a slight increase in CNR for TR between 300 and 900 ms. The CNR for opposed-phase imaging increased in a logarithm-like way with an increase in TR with saturation for longer TR values (ca. 900 ms), whereas for SE sequences there was a pronounced increase for CNR to a maximum (TR = 300 ms) with a nearly linear decline with increasing TR.

Similar to TR there was a logarithm-like increase in CNR for opposed-phase GE sequences with FA reaching a plateau with moderate drop for larger FA values. As a function of FA the maximum CNR was obtained for different TR values, increasing in FA for larger TR values (TR = 100 ms: FA = 30 °; TR = 500 ms: TR = 70 °; TR = 900 ms: FA = 90 °).

Similar general trends for variation of TR and FA were observed for in-phase GE sequences, although CNR values were substantially lower (Table 3). For 300 ms ≤ TR ≤ 900 ms and 30 ° ≤ FA ≤ 90 °CNR values for opposed-phase GE sequences were 1.68–3.71 the

Table 2. Contrast-to-noise ratios for red bone marrow and tumor metastasis for opposed-phase GE imaging (TE = 17 ms) as a function of TR and FA [$CNR_{(SE: TR/TE = 500/17 ms)} = 100$]

Flip angle (°)	Repetition time (ms)				
	100	300	500	700	900
10	84.9	87.1	87.6	87.1	87.1
30	143.3	209.9	230.5	240.2	240.2
50	124.4	245.1	301.9	331.7	350.0
70	93.6	230.5	318.7	354.9	366.8
90	73.0	201.3	290.5	346.3	386.3

Table 3. Contrast-to-noise ratios for red bone marrow and tumor metastasis for in-phase GE imaging (TE = 14 ms) as a function of TR and FA [$CNR_{(SE: TR/TE = 500/17 ms)} = 100$]

Flip angle (°)	Repetition time (ms)				
	100	300	500	700	900
10	49.8	50.3	52.5	51.9	50.3
30	64.4	108.2	128.2	138.0	142.8
50	34.1	114.2	152.6	175.8	191.0
70	3.2	81.7	142.3	185.6	207.2
90	–14.1	54.1	119.0	168.3	184.5

Table 4. Contrast-to-noise ratios for red bone marrow and tumor metastasis for spin-echo imaging as a function of TR [$CNR_{(SE; TR/TE = 500/17 ms)} = 100$]

Echo time (ms)	Repetition time (ms)				
	100	300	500	700	900
14	–108.7	–174.5	–125.5	–80.9	–32.7
17	–93.6	–144.2	–100.0	–65.7	–19.5

values of in-phase GE sequnces, with a general increase in CNR for higher FA and lower TR.

Compared with SE sequences with identical TR, CNR for opposed-phase GE sequences with FA = 90° was opposite in sign and substantially larger than for SE sequences (Tables 2, 4). For 300 ms ≤ TR ≤ 700 ms and 30° ≤ FA ≤ 90° CNR for GE sequences was 1.46–5.58 the values of corresponding SE sequences, with a pronounced increase for higher TR values and only a moderate influence of FA. This increase with TR was affected mostly by the decrease of contrast for SE sequences with prolongation of TR.

Discussion

Red bone marrow is composed of fat cells and hematopoietic cells. With GE sequences this macroscopic mixture of fat- and water-bound protons on cell-size basis within an imaging voxel ($Q_{F/W}$) can act as a sensitive imaging parameter for any kind of pathology disturbing the balance of fat- and water magnetization. In opposed-phase spoiled GE imaging the physiological cellular composition of red bone marrow results in a signal intensity reduction compared with in-phase imaging of at least 65% on the average [3]. As pathology without fat cells (tumors, inflammatory disease) or an increase in extracellular water (edema) causes a $Q_{F/W}$-related increase in signal intensity as compared with red bone marrow, contrast is greatly enhanced. These changes in signal intensity regularly are larger than those due to differences in relaxation times and proton density between pathology and red bone marrow.

The dominance of the influence of chemical shift over T2 or T2* for SE and GE sequences is shown by the fact that the average signal intensity difference for fat- and water-equivalent tissues (e.g., tumor) due to transverse magnetization loss between in-phase (TE = 14 ms) and opposed-phase (TE = 17 ms) TE was 12.5 ± 1.8% for GE sequences (T2*) (100 ms ≤ TR ≤ 900 ms, 10° ≤ FA ≤ 90°) and 9.4 ± 1.6% for SE sequences (T2). Transverse-magnetization-related SE signal intensity loss thus was slightly smaller (same TE values as for GE sequences) than for GE sequences (T2 vs T2*). However, this signal intensity loss for both sequence types was much smaller compared with the combined signal loss due to T2* and chemical shift for red bone marrow for opposed-phase as compared with in-phase GE sequences which was 69.3 ± 1.3% (100 ms ≤ TR ≤ 900 ms, 10° ≤ FA ≤ 90°).

The basis for the increase in sensitivity for opposed-phase GE sequences compared with SE sequences is the low signal intensity of red bone marrow and a pronounced increase in signal intensity for any shift in chemical composition regarding fat- and water-bound protons and thus fat cells and water-equivalent cells. In this respect it is irrelevant whether water-equivalent cells are replaced by fat cells as in replacement of red bone marrow by yellow bone marrow fat cells, or fat cells are replaced by water-equivalent cells as is typical for inflammatory disease or tumors, or the water-bound proton fraction is increased by edema.

Imaging experience with GE sequences and a TR ≥ 100 ms show that fat- and water-equivalent cells are characterized by a similar specific signal intensity. This results in a $Q_{F/W}$ for zero signal intensity close to 50/50 as mandatory for low signal intensity imaging of red bone marrow. In this case replacement of fat cells by water-equivalent cells (inflammatory disease, tumors, edema), or vice versa (fat cells), results in a signal intensity increase of comparable size. From this point of view the relatively narrow range of $Q_{F/W}$ ($40/60 < Q_{F/W} < 60/40$) centered at $Q_{F/W} = 50/50$ is the basis for low-signal-intensity GE imaging of red bone marrow. Our results in histological evaluation of red bone marrow specimens show that $Q_{F/W}$ in the majority of cases is in between $40/60 < Q_{F/W} < 60/40$. Literature reports on the fat content of red bone marrow vary. Snyder et al. [4] report a 40% amount of fat, Wismer et al. [1] a value of 35%. There is general agreement that the fat content increases with age. Dunnill et al. [5] report a decrease in hematopoietic cells from 57.9 ± 6.4% in the first decade to 34.5 ± 10.2% in the ninth decade. For the third to the ninth decade the relative amount of hematopoietic cells decreased from 39.6 ± 8.8% to 34.5 ± 10.2%, which is in good agreement with the values found in our specimens.

Nevertheless, there can be pronounced intraindividual variation in composition of red bone marrow for different anatomical sites [6].

Signal intensity of red bone marrow in most cases is below 35% compared with in-phase GE imaging. This holds for the whole range of imaging parameters examined (TR 100–900 ms, FA 10–90°).

From Eq. (6) follows also that signal intensity differences and thus contrast between red bone marrow and pathology are not necessarily dependent on ideal imaging conditions of a zero signal intensity for red bone marrow. The crucial factor for the change in signal intensity is the change of $Q_{F/W}$ caused by pathology.

For a complete exchange of one cell line by the other (either fat- or water-equivalent cells) the fat-to-water ratio becomes either $Q_{F/W} = 0/100$ or $Q_{F/W} = 100/0$. In this case, which is typical for tumor invasion, the maximum signal intensity change occurs ($D \rightarrow A > C \rightarrow A > B \rightarrow A$, $D \rightarrow G > E \rightarrow G > F \rightarrow G$) (Fig. 5). Signal intensity and thus contrast is larger the lower the signal intensity of intact red bone marrow.

Limitations regarding a signal intensity increase and thus contrast due to pathology occur in cases where a lesion causes a change in $Q_{F/W}$ which crosses the zero value D of the signal intensity curve. Here the change in $Q_{F/W}$ causes both a decrease as well as an increase in signal intensity ($A \rightarrow E$, $A \rightarrow F$, $A \rightarrow G$, $B \rightarrow E$, $B \rightarrow F$, $B \rightarrow G$, $C \rightarrow E$, $C \rightarrow F$, $C \rightarrow G$, or the reverse) with an imaging relevant signal intensity which is the difference of both signal intensity changes. This results in a smaller signal intensity increase than for the changes discussed above, and in certain cases results even in a signal intensity decrease ($A \rightarrow E$, $A \rightarrow F$, $B \rightarrow F$, $G \rightarrow C$, $G \rightarrow B$, $F \rightarrow C$); in the worst case, although rare, it results in equal signal intensity of pathology to surrounding tissue ($B \rightarrow F$, $C \rightarrow E$, or the reverse).

For SE sequences $Q_{F/W}$-related changes in signal intensity are unambiguous. The change in $Q_{F/W}$ from fat- to water-equivalent protons results in a linear decrease in signal intensity. Apart from differences in relative signal intensity for the monosubstances the change is identical to in-phase GE sequences. For T1 SE sequences (different T1) there is pronounced signal intensity difference between fat- and water-equivalent tissues, especially low-signal-intensity pathology (A: $Q_{F/W} = 0/100$; G: $Q_{F/W} = 100/0$) by far exceeding the signal intensity difference for monosubstances imaged with opposed-phase and in-phase GE sequences ($TR \geq 100$ ms; $A \rightarrow G$, $G \rightarrow A$; Fig. 5).

An advantage of opposed-phase GE sequences over SE sequences is the almost identical specific signal intensity of fat cells and water-equivalent cells which results in isointense imaging of fat and muscle facilitating detection of pathology as only pathology and, depending on TR and FA, liquids present with high signal intensity.

The signal intensity for GE sequences is crucially dependent on the phase difference of the transverse fat- and water-magnetization. The fat-water cycle time for minimum or maximum signal intensity is shorter the higher the B_o. For $B_o = 1.5$ T the cycle time is 4.5 ms, whereas it is 34.0 ms for $B_o = 0.2$ T (Table 1). As TE for opposed-phase imaging is linearly related to the fat-water cycle time and the minimum phase shift for opposed-phase imaging is π (0.5 fat-water cycles), the minimum opposed-phase TE for low magnetic fields not only is much longer than for higher fields but may be too short for the shortest TE applicable for low field imagers, whereas the second opposed-phase TE at 1.5 fat-water cycles results in a pronounced signal intensity decay with a low signal-to-noise ratio and pronounced T2*-weighting.

Other limitations occur for high-field imagers. For $B_o = 1.5$ T the fat-water cycle time is 4.5 ms only, making it crucial to adjust TE exactly to opposed-phase $\Delta\varphi = \pi$. The increase in red bone marrow signal intensity due to phase errors is dependent on $Q_{F/W}$. For ideal imaging conditions with zero signal intensity of red marrow for the optimal TE, a TE error of 0.5 ms results in a signal intensity increase in red marrow equivalent to 35% of the in-phase signal intensity. For red marrow with a residual signal intensity of 20% of the in-phase signal intensity the resulting signal intensity is 40%; thus, there is a relatively lower increase than for the ideal $Q_{F/W}$. This example demonstrates that selecting a TE close to the ideal TE is crucial for low-signal-intensity imaging of red bone marrow.

Comparing the CNR for opposed-phase GE and SE sequences, there are substantial differences regarding the contrast between tumor and red bone marrow. Whereas for SE sequences there is negative contrast of the lesion, GE sequences are characterized by positive lesion-to-marrow contrast with high-signal-intensity imaging of pathology and low signal intensity of bone marrow.

For opposed-phase GE and SE sequences with identical TR there are also differences regarding an optimal range of acquisition parameters. For GE sequences there is a broader TR range for a CNR ≥ 80% of the maximum value than for SE sequences with $500 \text{ ms} \leq TR \leq 900 \text{ ms}$ and $50° \leq FA \leq 90°$ (TR = 500 ms: 70° only). For a CNR ≥ 50% this range extends to $300 \text{ ms} \leq TR \leq 900 \text{ ms}$ and $30° \leq FA \leq 90°$ (exception: TR = 300 ms, FA = 30°). This broad range increases flexibility regarding selection of TR values via the number of slices according to anatomical demands. For SE sequences a CNR ≥ 80% of the maximum value is obtained for TR = 300 ms only, and a CNR ≥ 50% for $100 \text{ ms} \leq TR \leq 500 \text{ ms}$.

For diagnostic demands where opposed-phase GE imaging is combined with SE imaging with an identical number of slices, TR values of 300 or 500 ms should be applied, where CNR for GE imaging with TR = 500 ms is 75% (FA = 90°) and 86% (FA = 50°) of the maximum or for imaging with TR = 300 ms is 52 and 70%, respectively. The corresponding numbers for SE sequences are 69 and 100%.

For the whole diagnostically recommended TR and FA range opposed-phase GE sequences offer a CNR superior to SE sequences (opposite in sign). Compared with SE sequences with TR = 300 ms (TE = 17 ms), the CNR of GE sequences for the TR and FA range of

CNR values ≥ 80 % of the maximum value are between 2.21 and 2.68, for TR = 500 ms between 3.19 and 3.86, and for TR = 700 ms between 4.85 and 5.88. For the opposed-phase CNR, TR and FA range with ≥ 50 % of the maximum value between 1.40 and 2.68, 2.01 and 3.86, and 3.06 and 5.88, respectively. This demonstrates sensitivity of opposed-phase GE imaging for diagnosis in red bone marrow pathology.

References

1. Wismer GL, Rosen BR, Buxton R, Stark DD, Brady TJ (1985) Chemical shift imaging of bone marrow: preliminary experience. Am J Roentgenol 145: 1031–1037
2. Hidajat N, Hosten N, Sander B, Felix R (1995) Quantifizierung der Signalmodulation des blutbildenden Knochenmarkes in Gradienten-Echo-Sequenzen. Fortschr Rontgenstr 162: 145–151
3. Seiderer M, Wagner H, Stäbler A, Fink U (1994) Kernspintomographische Diagnostik fokaler Läsionen des roten Knochenmarks. Fortschr Rontgenstr 160: 453–458
4. Snyder WS, Cook MJ, Nasset ES, Karhausen LR, Howells GP, Tipton IH (1974) International Commission on Radiological Protection. Report of the task group on reference man. Pergamon Press, New York, pp 79–98
5. Dunnill MS, Anderson JA, Whitehead R (1967) Quantitative histological studies on age changes in bone. J Pathol Bacteriol 94: 275–291
6. Hartsock RJ, Smith E, Petty CS (1965) Normal variations with aging of the amount of haematopoietic tissue in bone marrow from the anterior iliac crest. Am J Clin Pathol 43: 326–331

Book review

European Radiology

Greenspan A., Remagen W.: Differential diagnosis of tumors and tumor-like lesions of bones and joints. Philadelphia, New York: Lippincott-Raven Publishers, 1998, 435 pages, 1047 illustrations, £ 258.00, ISBN 0-397-51710-6

The main purpose of this new work on benign and malignant bone lesions and lesions situated around or in the joint is to facilitate the process of differential diagnosis of these lesions for the radiologist and the pathologist. Since the radiologic and pathologic processes of differential diagnosis are frequently completely different, the two diagnostic approaches are discussed separately.

One of the master chapters of this book is the first one, entitled 'Radiologic and pathologic approach to bone tumors.' An analytic approach to the evaluation of bone lesions is given with reference to all the parameters of diagnostic or differential diagnostic value: patient age, multiplicity of a lesion, its location in the skeleton and in a particular bone, and the radiographic morphology. The analysis of the radiographic morphology is well stressed, including the evaluation of the borders of the lesion, the type of bone destruction, periosteal response, type of tumor matrix, and the possible soft tissue mass. All the clues for a correct analysis are perfectly explained in this chapter. Clear differential diagnostic messages, combining simplicity with top-level education, are illustrated in several schemes, drawings, and images. The role of each imaging modality in diagnosis, differential diagnosis, and staging is well determined.

The next eight chapters are dedicated to the different types of lesions: bone-forming tumors, tumors of cartilaginous origin, fibrous and fibrohistiocytic lesions, round cell lesions, vascular lesions, miscellaneous tumors and tumor-like lesions, metastases, and tumors and tumor-like lesions of the joints. Major lesions discussed in the chapter 'Miscellaneous tumors and tumor-like lesions' are the benign giant-cell tumor, simple bone cyst and aneurysmal bone cyst, and the malignant adamantinoma and chordoma.

In 'Tumors and tumor-like lesions of the joints' synovial (osteo)chondromatosis, pigmented villonodular synovitis, nodular tenosynovitis, synovial hemangioma, synovial sarcoma, and synovial chondrosarcoma are covered.

Each of these chapters provides information concerning clinical presentation of the lesion, imaging techniques and radiologic features, histopathology, and radiologic and pathologic differential diagnosis. The chapters are richly illustrated with good-quality roentgenograms, CT and MR images, beautiful color photomicrographs, and schematic drawings. The typical as well as the atypical features of each lesion are discussed.

Important diagnostic features are provided in concise tables, and the summary of differential diagnosis is included at the end of each section in the form of a schematic drawing, which also depicts the less likely differential possibilities. All major lesions are accompanied by drawings of a skeleton depicting the common and less common distribution of the lesion. All these schemes, tables and drawings are of outstanding clarity and didactic value. Detailed and up-to-date references are provided at the end of each chapter.

The text has been written with the radiologist and pathologist in mind, but the book is also useful for the orthopedic oncologist as well as other physicians. Radiologic imaging forms the major part of the illustrations although the histologic aspect is sufficiently well covered.

Since the book focuses on diagnosis and differential diagnosis, little attention has been paid to the local staging of lesions. Their treatment is beyond the scope of this work.

The major qualities of this book are its outstanding didactic level, its unequalled interest in differential diagnosis, and its well-balanced and richly illustrated combination of radiologic and pathologic information, written in an agreeable and fluent style. Because of these qualities this work by far is the most usable in daily practice. I can highly recommend it as a future standard work to all radiologists dealing with diagnosis of tumors and tumor-like lesions of bones and joints. They need to be aware of the importance of high-quality radiologic differential diagnosis, since not infrequently only the combination of radiologic and pathologic analysis leads to the correct diagnosis.

P. Brys, Leuven